

## FAST PULSED REACTORS FOR NEUTRON PHYSICS EXPERIMENTS

I.M.Frank, V.I.Luschikov and E.I.Sharapov

Laboratory of Neutron Physics, Joint Institute for Nuclear  
Research, Dubna, Head Post Office Box 79, 101000 Moscow,  
USSR

**Abstract:** Fast pulsed reactors IBR-2 and IBR-30 are in routine use in the Laboratory of Neutron Physics, JINR, Dubna. Their today characteristics and performances are reported. The IBR-2 in use for condensed matter research is mentioned. Some results of nuclear physics experiments conducted during the recent years at the IBR-30 reactor working with a linear accelerator as an injector are reviewed. The fields of research under discussion are : p-wave neutron resonance spectroscopy and parity nonconservation; differential scattering cross sections and p-wave neutron strength functions; cascade  $\gamma$ -transitions and peculiarities of the nuclear structure; prompt  $\gamma$ -ray yields and characteristics of the U-235 fission induced by resonance neutrons.

(neutron sources, pulsed reactors, polarized neutrons, parity violation, neutron scattering, strength functions, gamma-ray spectrum, nuclear structure, fission gamma-rays, fission fragments)

Introduction

Two periodically pulsed reactors IBR-30 /1/ and IBR-2 /2/ are in routine use in the Laboratory of Neutron Physics of the Joint Institute for Nuclear Research in Dubna, USSR. They are designed for fundamental and applied research in the field of neutron physics by the time-of-flight method. The IBR-30 was put into operation in June 1969, its design average thermal power being 30 kW. The IBR-2 reactor has been working at an average power of 2 MW since 1984. It is the most powerful source of pulsed neutrons for condensed matter research. One may find recent reviews of this field in the contributions to the Jamada Conference /3/ and Alushta School /4/. Now the reactor IBR-30 is in use for nuclear physics experiments only. Some of the reviews of these activities, for example, that given in /5/ are out of date. This talk is intended to cover the new physical results which have recently been obtained at the IBR-30.

Reactor Characteristics as for 1988

The IBR-2 is the pulsed reactor with liquid sodium as a coolant. The pulsed thermal power is 1500 MW, pulse duration being  $215 \pm 4$   $\mu$ sec and pulse repetition rate 5 p.p.s. The instantaneous thermal neutron flux from the surface of moderators reaches  $10^{16}$   $\text{cm}^{-2}\text{s}^{-1}$ , the total yield of fast neutrons is  $10^{17}$   $\text{s}^{-1}$ . The experiments are conducted on 11 neutron beams using various spectrometers such as the diffractometers, inelastic scattering and small angle scattering spectrometers, special set-up for the polarization analysis, etc.

The IBR-30 is the pulsed reactor of the first generation, air cooled. Today it is working only in a booster mode of operation by multiplying the neutrons generated in the tungsten target of the linac. The maximum energy of the linac is 40 MeV, the pulsed current is 0.4 A, the pulse duration is 1.7  $\mu$ sec at a repetition rate of 100 p.p.s. The width of the reactor power pulse in this regime is 4.5  $\mu$ sec at the multiplication of 200. The total neutron yield amounts to  $5 \times 10^{14}$   $\text{s}^{-1}$ . Eight flight tubes are in use. The spectral density of resonance neutrons is

$$\rho(E) = \frac{2.7 \times 10^7}{E^{0.9} L^2} \text{ cm}^{-1} \text{ eV}^{-1} \text{ s}^{-1}, \quad (1)$$

where E is the neutron energy in eV and L is the flight path in meters.

Polarized Neutrons, Parity Nonconservation in Neutron Resonances

Polarized resonance neutrons were made available by the proposal of their transmission through a dynamically polarized proton filter /6/. The method was first realized in Dubna with many investigations with polarized neutrons to follow /7/. At the beginning of the 80's large parity violation effects in the resonances of  $^{117}\text{Sn}$ ,  $^{81}\text{Br}$ ,  $^{111}\text{Cd}$  and  $^{139}\text{La}$  were discovered /8/. The question is of the helicity dependence of neutron cross section  $\sigma(E)$

$$\sigma(E) = \sigma_0(E) [1 + \mathcal{P}(\vec{\epsilon} \cdot \vec{k})], \quad (2)$$

where  $\vec{k}$  is the unit vector in the direction of the neutron momentum.  $\vec{\epsilon}$  is the spin unit vector and  $\mathcal{P}$  is the measure of the effect. The largest  $\mathcal{P}$ -value was found in the p-resonance of Lanthanum at  $E_p = 0.75$  eV,  $\mathcal{P} = (7.3 \pm 0.5) \times 10^{-2}$ . Several laboratories have joined this field of research in the recent years and confirmed some of the Dubna results /9,10,11/.

Recently a new search for the weak low energy p-wave resonances has been undertaken at Dubna. The resonances at  $E_p = 7.0$  eV and 4.9 eV in the targets of  $^{113}\text{Cd}$  and  $^{141}\text{Pr}$  were found. The helicity dependence of the total neutron cross section for these resonances as well as for the known resonances of  $^{93}\text{Nb}$  was measured. The following  $\mathcal{P}$ -values were obtained (in  $10^{-3}$  units) :  $3.7 \pm 5.2$  (7.0 eV  $^{113}\text{Cd}$ ),  $2.5 \pm 1.7$  (4.9 eV  $^{141}\text{Pr}$ ),  $-0.9 \pm 1.2$  (35.8 eV  $^{93}\text{Nb}$ ),  $0.9 \pm 1.7$  (42.2 eV  $^{93}\text{Nb}$ ) /12/. The effects if exist are below the experimental accuracy.

It is necessary to have in mind that the parity violation effects may be suppressed by the mixing parameter  $\alpha = \Gamma_{n1/2} / \Gamma_n$ , where  $\Gamma_n$  is the total neutron width ( $\Gamma_n = \Gamma_{n1/2} + \Gamma_{n3/2}$ ) which is the combination of the widths with the total angular momentum  $j = 1/2$  or  $3/2$ . The mixing parameter, neutron  $\Gamma_n$  and total width  $\Gamma$

for gamma-transitions with energy  $E_{\gamma i}$ , all of them must be determined to derive the weak interaction matrix element from the experiments. Reference /13/ has already reported about the first steps in this direction made in Dubna. Neutron gamma-correlations were measured in  $^{117}\text{Sn}$  including the fore-aft asymmetry for unpolarized neutrons and the analyzing power for capture of transversely polarized neutrons. Recently the  $\gamma$ -ray yields for direct transitions from the resonances in targets  $^{111}\text{Cd}$  and  $^{113}\text{Cd}$  were measured /14/. The parameters deduced are listed in the Table. The mixing parameter  $x$  has not been determined thus far. Additional measurements are necessary.

Table. Parameters of p-Wave Resonances

Nucleus	$E_p$ , eV	J	$g \Gamma_n$ , $10^{-7}$ eV	$\Gamma$ , meV	$E_{S1}$ , MeV	$\Gamma_{\gamma i}$ , meV
$^{117}\text{Sn}$	1.33	1	1.66(30)	180(18)	9.32	1.2(3)
$^{113}\text{Cd}$	7.00	1	3.10(30)	160(20)	9.04	4.5(9)
$^{111}\text{Cd}$	4.56	1	10.7(5)	163(10)	9.46	4.0(8)
$^{111}\text{Cd}$	6.95	0, 2	10.8(8)	143(13)	9.46	0

Neutron Scattering, p-Wave Neutron Strength Functions

Average differential elastic scattering cross sections for nuclei from the region  $48 \leq A \leq 144$  were measured. The neutron energy interval under study was from 20 to 300 keV. At such energies the contribution of p-wave to neutron cross section is weak. One may use the following decomposition

$$\sigma(\theta) = \left(\frac{G}{4\pi}\right) \left[ 1 + \omega_1 P_1(\cos\theta) + \omega_2 P_2(\cos\theta) \right], \quad (3)$$

where  $P_1(\cos\theta)$  and  $P_2(\cos\theta)$  are the Legendre polynomials,  $\omega_1$  and  $\omega_2$  are the parameters which are expressed in /15,16/ through neutron strength functions  $S^0$ ,  $S_{j^1}^1 = 1/2$ ,  $S_{j^1}^3 = 3/2$  and phases of the potential scattering. Undoubtedly these measurements are of value for applied sciences because of the contributed nuclear data. They led also to the physical results on spin-orbital effects in the neutron strength functions.

The possibility of splitting of the 3p-maximum of the neutron strength function was discussed long ago, but was not established with certainty. The authors of the work /15/ have done this. They have determined the p-wave strength functions  $S_{j^1}^1 = 1/2$  and  $S_{j^1}^3 = 3/2$  shown in Fig. 1 by analysing their data with the use of eq.(3). Open points are nuclei with an odd mass number  $A$ , others for even-even nuclei, the Lorentz curves are the fittings. Two different maxima are evidently present. The splitting is  $\Delta A = 12 \pm 4$ . The similar effect is found in the dependence of effective radii  $R_{1/2}^1$ ,  $R_{3/2}^1$  on the mass number.

Gamma-cascades, Nuclear Structure

New measurements of the two-quantum cascades following the radiative capture of thermal neutrons were performed recently. The gamma-spectrometer used consisted of two large Ge(LI) detectors of  $140 \text{ cm}^3$  each /17,18/. Figure 2 shows an example of the cascade spectrum  $I_{\gamma\gamma}$  obtained by the method of summation of amplitudes of coinciding pul-

ses. The corresponding summation spectrum is shown in Fig. 3, where  $N$  stands for the counts per channel and  $n$  is the channel's number. The figures over peaks in Fig. 2 correspond to the ray energies  $E_{\gamma}$  in keV and in Fig. 3 to the energies  $E_f$  of final states.

The total intensity  $I_{\text{calc}}$  of the cascade spectra may be calculated /19/ as

$$I_{\gamma\gamma}^{\text{calc}} = K \left[ \sum_{g=1}^n \frac{\Gamma_{Bg}(E_{\gamma}) \cdot \Gamma_{gf}(E_f - E_{\gamma})}{\Gamma_B \Gamma_g} + \sum_{h=1}^m \frac{\Gamma_{Bh}(E_f - E_{\gamma}) \cdot \Gamma_{hf}(E_{\gamma})}{\Gamma_B \Gamma_h} \right], \quad (4)$$

provided radiation widths and the level positions are known or a statistical model is employed.

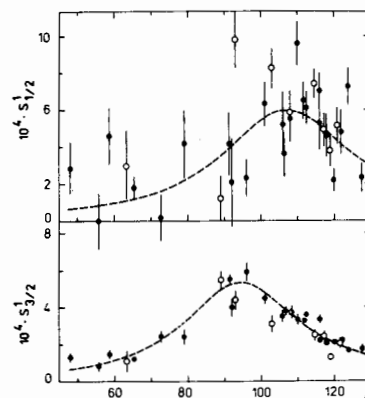


Fig. 1. The p-wave neutron strength functions versus mass number  $A$

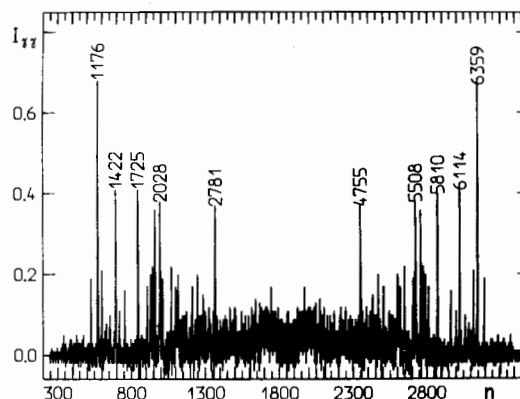


Fig. 2. The two-quantum cascade spectra from the  $^{177}\text{Hf}(n, \gamma)^{178}\text{Hf}$  reaction

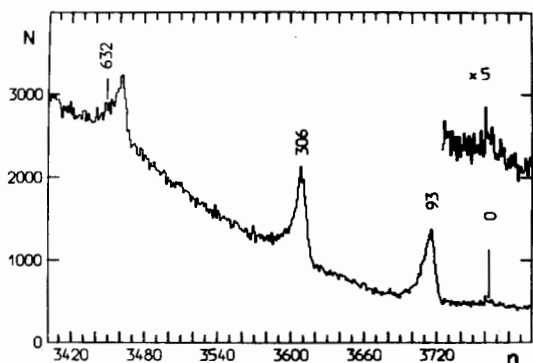


Fig. 3. The summation spectra from the  $^{177}\text{Hf}(n, 2\gamma)^{178}\text{Hf}$ .

In eq. (4) B means the neutron binding energy, g and h designate the intermediate levels, n the number of levels if a first quantum has the energy  $E_\gamma$ , m is the same in the case of a first quantum having the energy  $(E_f - E_\gamma)$ , the coefficient K is the normalization constant. The comparison between the  $I_{\text{calc}}$  and  $I_{\text{exp}}$  intensities gives way to a certain conclusion on the structure of nuclear levels connected by two-quantum cascades.

The results obtained for the rare-earth nuclei are presented in Ref. /19/. As a rule  $I_{\text{calc}}$  and  $I_{\text{exp}}$  differ from each other. For example, in the case of the  $^{175}\text{Yb}$  and  $^{179}\text{Hf}$  product nuclei those groups of cascades are intensified which have the intermediate energy values near to the positions of one-quasiparticle states of a deformed Saxon-Woods potential; in the case of the  $^{168}\text{Er}$  and  $^{187}\text{Hf}$  nuclei similar effects are connected with the structure of the final states which are the one-phonon states as a rule. Moreover, the intense cascades are correlated with the neutron width of the resonances which dominate the capture cross section at thermal energies. The results are interpreted as the increase of partial  $\gamma$ -widths due to the existence of large one-quasiparticle components in all three levels connected by two quantum cascades. The level schemes

in the energy range up to 3 MeV are also presented in Ref. /19/.

#### Gamma-Rays from $^{235}\text{U}$ Fission Induced by Resonance Neutrons

An appropriate experimental apparatus was installed at the Laboratory of Neutron Physics, JINR, to study the mass and charge distributions for the  $^{235}\text{U}$  fission induced by resonance neutrons. It consisted of a fast ionization chamber (10 g  $^{235}\text{U}$ ) and Ge(Li) spectrometer working in coincidence /20/. The beam of resonance neutrons at a distance of 57 m from the IBR-30 booster was used for the measurements in the neutron energy interval from 0.7 eV to 36 eV with the resolution 70  $\mu\text{eV}$ . Prompt  $\gamma$ -yields from excited states of some fission fragments were measured by the time-of-flight method. Figure 4 shows as an example the time-of-flight spectrum which corresponds to the registration of the 199 keV quanta from the  $^{144}\text{Ba}$  fragment. The figures over resonances are the energies in eV.

The preliminary results obtained with this technique are given in Ref. /21/. Gamma-yields from  $^{95}\text{Sr}$ ,  $^{100,102}\text{Zr}$  and  $^{142,144,146}\text{Ba}$  fragments were compared with other fission characteristics (obtained in different laboratories) such as the average kinetic energy, neutron multiplicity, fragment angular anisotropy coefficients. Significant correlations between these characteristics have been found for 23 resolved resonances with  $J^\pi = 4^-$ . It is known that the channels with  $K=1$  and  $K=2$  dominate in such resonances and one may introduce a quantity  $P_\lambda = \frac{\Gamma_{\lambda f}^{K=1}}{\Gamma_{\lambda f}^{K=1} + \Gamma_{\lambda f}^{K=2}}$

to characterize a relative openness of the channel with  $K=1$  in a given resonance  $\lambda$ . In Ref. /21/ it was observed that many characteristics under study correlate with  $P_\lambda$ , see, for example Fig. 5. This means that the admixture of the vibration fission states with fixed J K values influences the fission induced by resonance neutrons.

#### Summary

Nuclear Physics experiments of the Laboratory of Neutron Physics in Dubna are conducted with the aid of the pulsed reactor IBR-30 working in the booster mode of operation. They are the time-

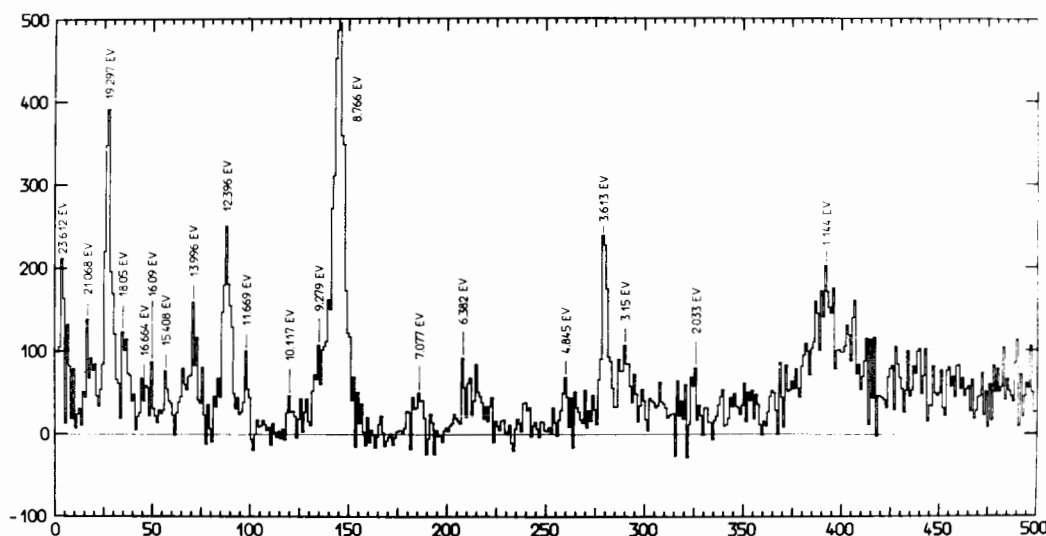


Fig. 4. The time-of-flight spectrum of fission resonances in  $^{235}\text{U}$

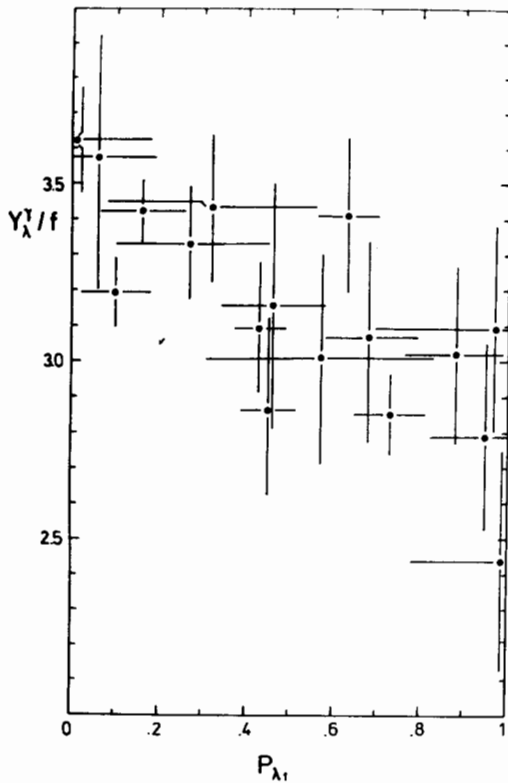


Fig. 5. The  $\gamma$ -quanta yields ( $E = 212$  keV) from  $^{100}\text{Zr}$  fragment) from  $^{235}\text{U}$  resonances in dependence on parameter  $P_\lambda$ .

of flight experiments in the field of high intensity neutron spectroscopy at moderate resolution. New directions of research which exploit original experimental techniques and apparatuses created in the last few years are briefly reviewed. These experiments are under further development.

#### References

1. I.M.Frank. Problems of Physics, Sov.J. Nucleus and Particles, **2**, 807 (1972), in Russian.
2. V.D.Ananiev et al. Sov. J. Atomic Energy, **57**, 227 (1984), in Russian.
3. I.M.Frank, P.Pacher, Neutron Scattering in Condensed Matter, VI Hakone, Japan, 1982 (North Holland, Amsterdam, 1983).
4. Yu.M.Ostanevich, V International School on Neutron Physics, Alushta, 1986. (JINR D3,4, 17-86-747, Dubna, 1987)p.221.
5. V.I.Luschikov et al. Nuclear Cross Sections for Technology, ed. J.L.Fowler, C.H.Johnson, C.D. Bowman (NBS Special Publication 594, Washington, 1980) p.385.
6. Yu.V.Taran, F.L.Shapiro, ZhETF, **44**, 2185 (1963) in Russian.
7. V.P.Alfimenkov et al. Nucl.Phys. **A376**,229(1982).
8. V.P.Alfimenkov et al. ZhETF Lett. **34**, 295 (1982) Nuclear Data for Science and Technology, ed. K.H.Bockhoff (Reidee, Dordrecht, 1983) p.773.
9. S.A.Biryukov et al. Sov.J. Nucl.Phys. **45** 1511 (1987).
10. Y.Masuda et al. Tests of Time Reversal Invariance in Neutron Physics, eds. N.R. Gould, J.D.Bowman (World Scientific, Singapore, 1987) p.191.
11. C.Bowman. New Neutron Physics using Spallation Sources, these Proceedings.
12. V.P.Alfimenkov et al. JINR P3-87-43, Dubna (1987) in Russian.
13. V.P.Alfimenkov et al. Nuclear Data for Pure and Applied Science, eds. P.G.Young, R.E.Brown, G.F.Auchampaugh, P.W.Lisowski, L.Stewart (Gordon and Breach, N.Y. 1986) p.937.
14. V.P.Alfimenkov et al. JINR P3-87-117, Dubna (1987) in Russian.
15. A.B.Popov, G.S.Samosvat, Rapid Communications JINR N18-86, Dubna (1986) p.30, Sov.J. ZhETF Lett. **38**, 304 (1983) in Russian.
16. L.V.Kuznetsova, A.B.Popov, G.S.Samosvat, JINR P3-87-393, Dubna (1987), in Russian.
17. A.M.Sukhovoij, V.A.Khitrov, Sov.J. PTE, No.5, 27 (1984). A.A.Bogdzal et al. JINR P15-82-706, in Russian.
18. S.T.Boneva, E.V.Vasilieva, A.M.Sukhovoij, JINR P6-87-98, Dubna (1987), in Russian.
19. S.T.Boneva et al. JINR P3-87-513, Dubna (1987), Z.Phys.A (1988) to be published.
20. J.Kliman et al. Acta Physica Slovaca, **36**, 245, (1986).
21. N.A.Gundorin et al. JINR P3-87-718, Dubna (1987).